Korean Chem. Eng. Res., 55(6), 868-873 (2017)
https://doi.org/10.9713/kcer.2017.55.6.868
PISSN 0304-128X, EISSN 2233-9558

On Compositional Convection in Near-Eutectic Solidification System Cooled from a Bottom Boundary

In Gook Hwang†

Department of Chemical Engineering, The University of Suwon, 17, Wauan-gil, Bongdam-eup, Hwaseong, Gyeonggi, 18323, Kroea
(Received 20 June 2016; Received in revised form 22 August 2016; accepted 24 August 2016)

Abstract – Natural convection is driven by the compositional buoyancy in solidification of a binary melt. The stabilities of convection in a growing mushy layer were analyzed here in the time-dependent solidification system of a near-eutectic melt cooled impulsively from below. The linear stability equations were transformed to self-similar forms by using the depth of the mushy layer as a length scale. In the liquid layer the stability equations are based on the propagation theory and the thermal buoyancy is neglected. The critical Rayleigh number for the mushy layer increases with decreasing the Stefan number and the Prandtl number. The critical conditions for solidification of aqueous ammonium chloride solution are discussed and compared with the results of the previous model for the liquid layer.

Key words: Compositional convection, Solidification, Mushy layer, Ammonium chloride solution

1. Introduction

In the solidification system of a binary alloy a mushy layer forms between the melt and the solid layer. The mushy layer is a two-phase region of dendritic crystals and the residual liquid. Thermal and compositional fields develop in the liquid and mushy layers and compositional convection can be induced by the buoyancy force due to an unstable density profile. Compositional convection in a mushy layer causes freckles in the resultant solid and deteriorates the quality of solid products in the materials processing, such as the crystal growth [1-5]. Natural convection in the mushy layer during directional solidification is observed in the experiments of aqueous ammonium chloride solution [6,7]. In the liquid layer, convection is unstable first in the solutal boundary layer above the liquid-mushy interface. When the mushy-layer mode of convection occurs, convective plumes rise into the liquid region from chimneys in the mushy layer [8].

Emms and Fowler [9] employed a quasi-static stability analysis in the solidification of binary alloys and investigated the onset of convection in a mushy layer using the model for a finger-like convection in the liquid layer. Choi *et al*. [10] and Kim and Choi [11] analyzed the stabilities of thermal convection in a fluid layer and in a porous layer saturated with liquid using propagation theory. This theory uses a length scale that is proportional to the thermal penetration depth, i.e., the square root of time. Propagation theory predicts a larger onset time for the time-dependent heating fluid layer, compared to the convectional frozen-time method that assumes the time-dependent basic state to be frozen and considers the time as a parameter in linear stability analysis.

We applied propagation theory to the solidification of the mushy layer in aqueous ammonium chloride solution. The onset of convection in the mushy layer solidifying impulsively from the bottom boundary was investigated and the self-similar stability equations were used for the liquid and mushy layers [12-16]. The critical conditions for compositional convection during time-dependent solidification were found numerically. In the mushy layer the simple model for solidification of a near-eutectic melt was used [9,12,15]. In the liquid layer the compositional boundary-layer and the thermal buoyancy were neglected [14,16]. The critical conditions for aqueous ammonium chloride solution were discussed, and the critical Rayleigh numbers were compared with the results from Emms and Fowler's [9] model for the liquid layer.

2. Governing Equations

The present study assumes that the initial composition of the solution is close to the eutectic composition. Consider the liquid and mushy layers in time-dependent solidification of a near-eutectic melt cooled from a bottom boundary (Fig. 1). The binary melt is initially quiescent at a temperature T_∞ and a composition of the less dense component C_∞. At time $t = 0$ the melt is cooled impulsively from below, and the mushy layer grows upwards with time. The liquid-mush interface H(t) is assumed to be planar. The mush-solid interface is at a eutectic temperature T_E and a eutectic composition C_E [12-16].

The dimensionless governing equations in the mushy layer during solidification of a near-eutectic melt are given by [9,12,15]

$$(1+S)\left(\frac{\partial}{\partial\tau}+\mathbf{u}\cdot\nabla\right)c=\nabla^2 c \tag{1}$$

† To whom correspondence should be addressed.
E-mail: ighwang@suwon.ac.kr

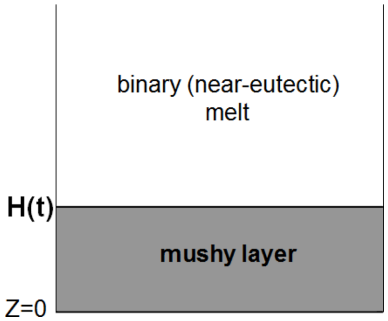

Fig. 1. Schematic diagram of time-dependent solidification of near-eutectic melt.

$$\mathbf{u} = -\nabla p + R_m c \mathbf{e}_k \tag{2}$$

$$\nabla \cdot \mathbf{u} = 0 . \tag{3}$$

The variables are defined as follows:

$$(x, y, z) = \frac{(X, Y, Z)}{L}, \ \mathbf{u} = \frac{L}{\kappa}\mathbf{U}, \ \tau = \frac{\kappa}{L^2}t \tag{4a~c}$$

where $\mathbf{e}_k$ is the unit vector in the *z*-direction, *L* is the characteristic length scale, *g* is the gravity acceleration, κ is the thermal diffusivity, and μ is the viscosity. And **u** is the dimensionless velocity and τ is the dimensionless time. The dimensionless pressure *p* is scaled with μκ/Π, where Π is the permeability in the mushy layer, and Π is assumed to be constant. The dimensionless temperature and composition are defined as

$$\theta = \frac{T - T_L(C_\infty)}{T_L(C_\infty) - T_E}, \ c = \frac{C - C_\infty}{C_E - C_\infty}, \ \theta = -c \tag{5a~c}$$

The liquidus temperature far in the melt is defined by $T_L(C_\infty) = T_0 - \Gamma C_\infty$, where T_0 is the melting point of the solvent and Γ is the slope of the liquidus curve. The Stefan number is defined by $S = L/C_P \Gamma C_\infty$, where $\overline{L}$ is the latent heat of fusion and C_P is the specific heat. The Rayleigh number for the mushy layer is defined as

$$R_m = \frac{g\beta_m \Delta C \Pi L}{\kappa \nu} \tag{6}$$

where ν is the kinematic viscosity. The effective expansion coefficient is defined by $\beta_m = \beta + \alpha\Gamma$, where α and β are the thermal and compositional expansion coefficients, respectively.

In the liquid layer the governing equations are considered in the limiting case of zero Lewis number (=D/κ), where D is the solute diffusivity. The compositional boundary-layer thickness is neglected and the compositional field is not considered in the liquid layer. And the thermal buoyancy force in the liquid layer is neglected. The governing equations in the liquid layer are given by [16]

$$\left(\frac{\partial}{\partial \tau} + \mathbf{u} \cdot \nabla\right)\theta = \nabla^2 \theta \tag{7}$$

$$\frac{1}{Pr}\left(\frac{\partial}{\partial \tau} + \mathbf{u} \cdot \nabla\right)\mathbf{u} = -\nabla p + \nabla^2 \mathbf{u} \tag{8}$$

$$\nabla \cdot \mathbf{u} = 0 \tag{9}$$

where *Pr* is the Prandtl number (=ν / κ).

The thermal-conduction state is assumed to be in the liquid and mushy layers. The basic-state governing equations are given by

$$\frac{d^2\theta_0}{d\zeta^2} + 2\lambda^2 \zeta \frac{d\theta_0}{d\zeta} = 0 \ \text{ for } \zeta > 1 \tag{10}$$

$$\frac{d^2 c_0}{d\zeta^2} + 2\lambda^2 \zeta (1+S) \frac{dc_0}{d\zeta} = 0 \ \text{ for } \zeta < 1 \tag{11}$$

where ζ (=z/2λ$\sqrt{\tau}$) is the similarity variable [12,15]. The phase-change rate λ has the relation of h = 2λ$\sqrt{\tau}$, where h is the depth of the mushy layer. The boundary conditions are

$$\theta_0 \to \theta_\infty \ \text{ for } \zeta \to \infty \tag{12}$$

$$\theta_0 = c_0 = 0 , \ \frac{\partial \theta_0}{\partial \zeta} = -\frac{\partial c_0}{\partial \zeta} \ \text{ at } \zeta = 1 \tag{13a,b}$$

$$c_0 = 1 \ \text{at} \ \zeta = 0 \tag{14}$$

The superheat θ_∞ is defined by

$$\theta_\infty = \frac{T - T_L(C_\infty)}{T_L(C_\infty) - T_E} \tag{15}$$

3. Stability Analysis

When linear stability theory is employed in the time-dependent heating or cooling fluid layer, the boundary-layer thickness is used as a length scale in the propagation theory. The time-dependent perturbation equations are transformed to functions of the similarity variable. In the present system the mushy-layer thickness *H* (=2λ$\sqrt{\kappa t}$) was used as a length scale, which is proportional to the square root of time. The self-similar stability equations for the marginal-stability state are expressed as [12-16]

in the mushy layer:

$$(\overline{D}^2 + 2(S+1)\lambda^2 \zeta \overline{D} - a^{*2})c^* = (S+1)R_m^* w_m^* \overline{D} c_0 \tag{16}$$

$$(\overline{D}^2 - a^{*2})w_m^* = -a^{*2} c^* \tag{17}$$

in the liquid layer:

$$(\overline{D}^2 + 2\lambda^2 \zeta \overline{D} - a^{*2})\theta^* = \frac{R_m^*}{Da^*} w^* \overline{D} \theta_0 \tag{18}$$

$$\left[(\overline{D}^2 - a^{*2})^2 + \frac{2\lambda^2}{Pr}(\zeta \overline{D}^3 - a^{*2}\zeta \overline{D} + 2a^{*2})\right] w^* = 0 \tag{19}$$

where $a^* = ah$, $R_m^* = R_m h$, and $\overline{D} = d/d\zeta$. The Rayleigh number R_m^* (=$g\beta_m \Delta C \Pi H/\mu\kappa$) and the wave number a^* are based on the mushy-layer thickness *H*. The Darcy number Da^* is defined as Π/H^2. In the mushy layer the concentration disturbance c^* has the scale of $\kappa\nu\Gamma / (g\beta_m L^3)$, and the velocity disturbance w_m^* has the scale of $\Pi\kappa/L^2$. In the liquid layer the temperature disturbance θ^* has the scale of $\kappa\nu\Gamma / (g\beta_m L^3)$, and w^* has the scale of $H^2\kappa/L^3$.

The following boundary conditions are applied to the self-similar

stability equations:

for $\zeta \to \infty$

$$\theta^* = 0, w^* = 0, \overline{D}\, w^* = 0 \quad (20a,b,c)$$

at $\zeta = 1$

$$\theta^* = -c^*, \overline{D}\theta^* = -\overline{D}c^* \quad (21a,b)$$

$$w^* = w_m^* Da^*, \overline{D}w^* = 0 \quad (21c,d)$$

$$\overline{D}w_m^* = -\left[\overline{D}w^* - 3a^{*2}\overline{D}w^* - \frac{2\lambda^2}{Pr}(\overline{D}w^* - \overline{D}^2 w^*)\right], \quad (21e)$$

at $\zeta = 0$

$$c^* = 0, w_m^* = 0 \quad (22a,b)$$

The no-slip condition is applied to the liquid on the liquid-mush interface [5]. The continuities of vertical velocity and pressure are applied at the liquid-mush interface.

The parameters a^* and R_m^* are assumed to be eigenvalues. The minimum value of R_m^* and its corresponding value of a^* are found numerically. The phase-change rate λ was obtained by solving the basic-state equations. We used the shooting method to solve the basic-state equations and the self-similar stability equations. For numerical integration of the self-similar stability equations we assumed the appropriate initial values at the liquid-mush interface. We used the Newton-Raphson iteration method to correct the assumed initial values.

4. Results And Discussion

In the present study the time-dependent solidification system was considered for a near-eutectic ammonium chloride solution. The dimensionless parameters are the superheat θ_∞, the Stefan number S, the Prandtl number Pr, and the Darcy number Da^*. The physical properties of aqueous ammonium chloride solution (NH_4Cl-H_2O) are $L = 3.14\times10^2$ kJkg^{-1}, $C_P = 3.25$ kJkg^{-1}K^{-1}, $\Gamma = 490$ K, and $c_E = 0.8$ [9]. For 26~28% NH_4Cl ($c_\infty = 0.72$~0.74) the parameters are assumed to be S=0.27, Pr=10, and $Da^* = 10^{-5}$.

Figure 2 shows the marginal-stability curves for various Prandtl numbers Pr for S = 0.27 and $\theta_\infty = 0.6$. The minimum value of the Rayleigh number R_m^* represents the condition for the onset of compositional convection in the mushy layer. The critical values for compositional convection were obtained as $R_{m,c}^* = 10$ and $a_c^* = 1.53$ for S=0.27 and $\theta_\infty = 0.6$. With decreasing Prandtl number the critical Rayleigh number $R_{m,c}^*$ increases and compositional convection in the mushy layer stabilizes. However, the change of $R_{m,c}^*$ between Pr=10 and 0.01 is not much (10%), since the compositional convection of the mushy-layer mode is not influenced sensitively by convection in the liquid layer. The Prandtl number Pr represents the ratio of the viscous diffusion rate to the thermal diffusion rate of the melt. In the present model we can obtain the critical conditions for the low Prandtl-number system, such as metal alloys. The Prandtl numbers are orders of 10^{-2}~10^{-1} in metallic alloys. The solidification system of metallic alloys is convectively more stable compared to the aqueous solution system.

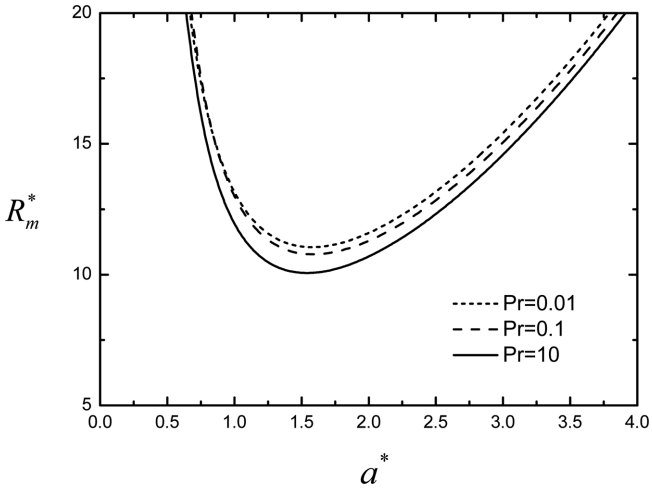

Fig. 2. Marginal-stability curves for various Prandtl numbers *Pr* with S = 0.27 and θ_∞=0.6.

In Emms and Fowler's [9] model the following equation is suggested for the liquid layer:

$$\frac{\partial\theta}{\partial\tau} + w_m\big|_{z=h}\frac{\partial\theta}{\partial z} = \nabla^2\theta \quad (23)$$

where $w_m|_{z=h}$ is the vertical velocity in the mushy layer at the liquid-mush interface. The upward flow from the mushy layer is included in the temperature field in the liquid layer based on the boundary-layer theory for a finger-like convection. This model considers the salt-finger convection above the liquid-mush interface and assumes that the boundary-layer mode of convection in the liquid layer little influences the onset of convection in the mushy layer. From Eq. (23) Hwang and Choi [12,15] derived the self-similar stability equation in the liquid layer:

$$(\overline{D}^2 + 2\lambda^2\zeta\overline{D} - a^{*2})\theta^* = R_m^* w_m^*\big|_{\zeta=1}\overline{D}\theta_0 \quad (24)$$

with the boundary conditions Eq. (20a) for $\zeta\to\infty$, (21a,b) at z=1, and (22a,b) at z=0. The permeable velocity condition ($\overline{D}w_m^* = 0$ at z=1) is applied at the liquid-mush interface. The liquid-mush interface was assumed to be planar and the disturbances at the interface were not considered. The deformable liquid-mush interface was studied by Hwang and Choi [12].

In Eq. (24) the momentum equation is not used in the liquid layer, while in the present model (Eqs. (18) and (19)) the convective motion is considered and the Prandtl number is included in the momentum equation. The marginal-stability curves from Eq. (24) for various values of the Stefan number S are shown in Fig. 3. Numerical results give the critical values of $R_{m,c}^* = 9.53$ and $a_c^* = 1.53$ for S = 0.27 and $\theta_\infty = 0.6$ ($\lambda = 0.606$). When $\theta_\infty = 0.6$, the critical Rayleigh number from Eq. (24) is 5 % smaller than that from Eqs. (18) and (19). The critical Rayleigh number $R_{m,c}^*$ decreases with increasing S, and the critical wave number a_c^* slightly increases with increasing S. The

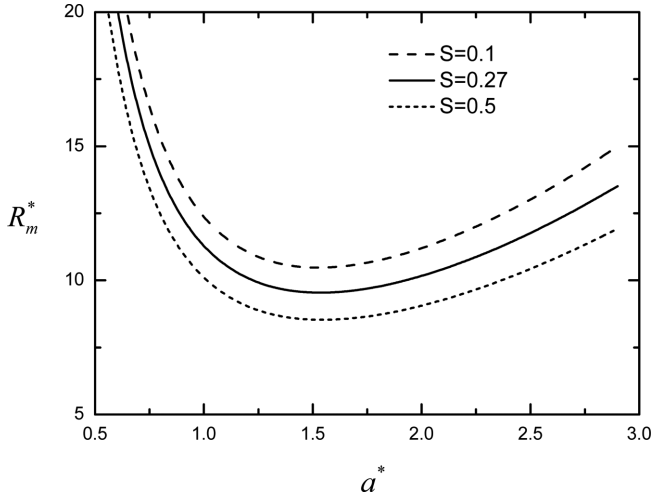

Fig. 3. Marginal-stability curves obtained by using Eq. (24) derived from Emms and Fowler's [9] model for various values of Stefan number S and θ_∞=0.6.

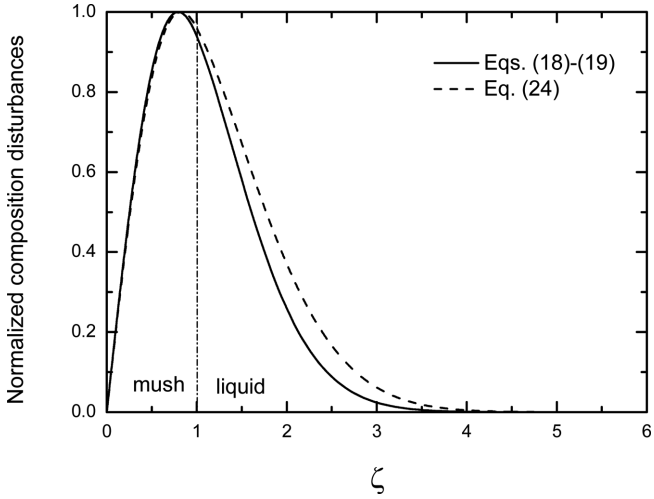

Fig. 5. Distributions of normalized composition disturbances in mushy layer and temperature disturbances in liquid layer for S = 0.27, Pr=10, and θ_∞=0.6.

Stefan number *S* is proportional to the ratio of the latent heat to the specific heat of the melt. When the material with the larger latent heat solidifies, the system is more unstable to the compositional convection. With increasing *S* the phase-change rate λ decreases (λ = 0.619 for S = 0.1 and λ = 0.590 for S = 0.5) and the basic compositional profile becomes more linear. The system is more stable for a curved compositional profile with a small boundary-layer thickness in the mushy layer than the linear one.

In Figs. 4 and 5 the present results from Eqs. (18)~(19) are compared with the model of Eq. (24) from Emms and Fowler [9]. These figures show the distributions of velocity and composition disturbances, which is normalized by its maximum absolute value, at the critical conditions for St = 0.27 and θ_∞ = 0.6. The velocity disturbances in the mushy layer show almost no differences between the two models though the momentum equation in the liquid is not considered in the model of Eq. (24). And the maximum point of velocity disturbances is at the liquid-mush interface. Therefore, the permeable velocity condition $\overline{D}w_m^*=0$ at the liquid-mush interface is a good approximation for a mushy-layer model. In a simple model of the mushy layer a constant-pressure boundary condition (permeable condition) is considered on the liquid-mush interface [17]. In Fig. 5 the composition disturbances in the mushy layer show no significant differences between the two models; however, the temperature disturbances in the liquid layer of the present model (Eqs. (18)~(19)) are more confined to the region on the liquid-mush interface than those of the model of Eq. (24). The gradient of the composition disturbances at the liquid-mush interface is different between the two models, and this difference influences the critical condition for the onset of convection. In the horizontal porous layer the critical Rayleigh number for an insulating boundary is smaller than that for a conducting boundary [18].

In Figs. 6 and 7, the present results of the critical conditions are

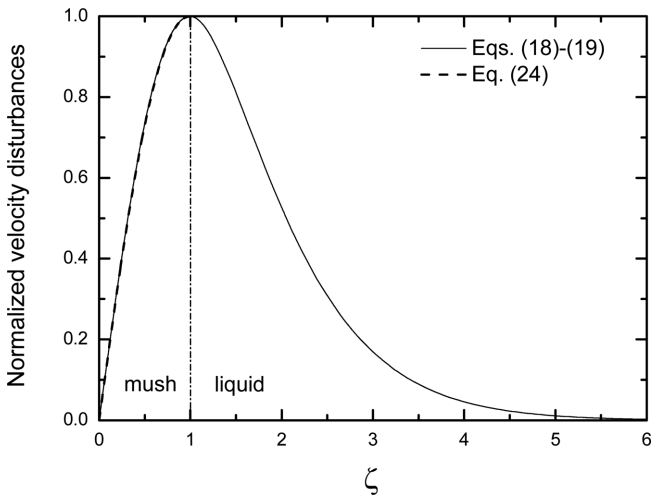

Fig. 4. Distributions of normalized velocity disturbances for S = 0.27, Pr=10, and θ_∞=0.6.

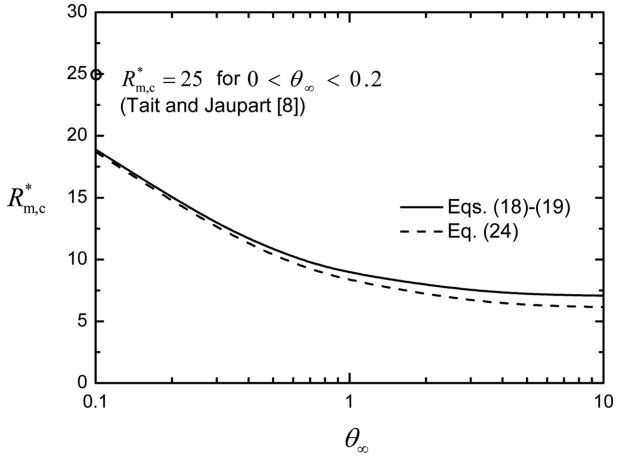

Fig. 6. Variation of critical Rayleigh number $R^*_{m,c}$ with superheat θ_∞ for S = 0.25 and Pr=10. Tait and Jaupart [8] obtained $R^*_{m,c}$ =25 for 0<θ_∞<0.2 in the experiment of solidification of aqueous ammonium chloride solution.

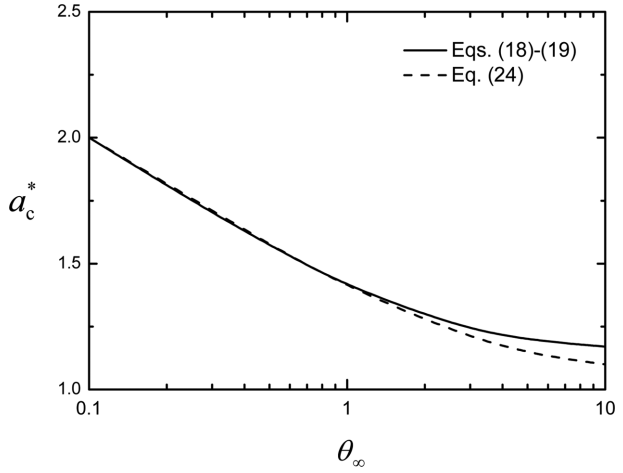

Fig. 7. Variation of critical wave number a_c^* with superheat θ_∞ for S = 0.25 and Pr=10.

compared with the model of Eq. (24) from Emms and Fowler [9]. They investigated the onset of convection in the mushy layer by employing a quasi-static analysis with $\partial(\cdot)/\partial\tau = 0$, which is a frozen-time model. They assumed the initial composition to be the eutectic one, that is, $c_\infty \approx 0.8$ and in this case S is approximately 0.25 for aqueous ammonium chloride solution. In Figs. 6 and 7, the critical values are plotted as a function of the superheat θ_∞ for S=0.25, Pr=10 and $Da^* = 10^{-5}$. The critical conditions $R_{m,c}^*$ and a_c^* decrease with increasing θ_∞, and $R_{m,c}^*$ approaches a constant value for a large value of θ_∞. The superheat θ_∞ represents the ratio of the temperature difference in the liquid layer to the temperature variation across the mushy layer. When the initial temperature of the melt is large, the superheat θ_∞ is large and the basic compositional profile is linear in the mushy layer. The superheat θ_∞ makes the solidification system of binary melts more unstable to the compositional convection in the mushy layer. The critical Rayleigh number $R_{m,c}^*$ obtained from the present model (Eqs. (18) and (19)) is larger than the model of Eq. (24). When θ_∞ is small ($\theta_\infty = 0.1$), the difference of $R_{m,c}^*$ between the two model is very small. For a small superheat θ_∞ the growth rate of the mushy layer is large and the temperature difference in the liquid layer is small. Tait and Jaupart [8] obtained the critical Rayleigh number for the mushy layer $R_{m,c}^* = 25$ for $0 < \theta_\infty < 0.2$ in the experiment of solidification of aqueous ammonium chloride solution. The experimental critical Rayleigh number for the onset of compositional convection in the mushy layer is 1.3 times larger than the present prediction. The critical wave numbers a_c^* are almost the same between the two model for $\theta_\infty \le 1$. Hwang and Choi [13] studied the onset of convection in the mushy layer and compared the critical conditions with existing theoretical and experimental results of aqueous ammonium chloride solution.

The relation for the phase change-rate as a function of θ_∞ is obtained from the interface condition (13b), i.e., $\partial\theta_0/\partial\zeta = -\partial c_0/\partial\zeta$ at $\zeta = 1$:

$$\lambda = \frac{\sqrt{\pi}}{2(\theta_\infty + 1)} \quad \text{for } \lambda \ll 1 \tag{25}$$

The phase-change rate λ approaches zero for an infinite θ_∞ and the asymptotic relation is $\lambda \sim \sqrt{\pi}/2\theta_\infty$ for $\theta_\infty \gg 1$ [9]. If θ_∞ is large, the growth rate of the mushy layer is very small and the time-dependency is weak.

When the superheat is very large ($\theta_\infty \to \infty$ and $\lambda \to 0$) the terms including λ, which is transformed from $\partial(\cdot)/\partial\tau$, are neglected. The self-stability equations in the mushy layer for $\theta_\infty \to \infty$ are given by

$$(\overline{D}^2 - a^{*2})c^* = (S+1)R_m^* w_m^* \overline{D} c_0 \tag{26}$$

$$(\overline{D}^2 - a^{*2})w_m^* = -a^{*2} c^* \tag{27}$$

These equations are similar to Emms and Fowler's [9] quasi-static stability analysis. In the mushy layer the basic composition profile is written as

$$c_0 = 1 - \frac{2}{\sqrt{\pi}\,\mathrm{erf}((1+S)^{1/2}\lambda)} \frac{(1+S)^{1/2}\lambda\zeta}{} + O(\lambda^2) \tag{28}$$

The formula $\sqrt{\pi}\,\mathrm{erf}(b) = 2b(1-\mathrm{erf}(b))$ for $b \ll 1$ was employed to produce the expansion $c_0 = 1-\zeta + O(\lambda^2)$ for $\lambda \ll 1$. Therefore, the gradients of the basic state become $\overline{D}c_0 = 1$ and $\overline{D}\theta_0 = -1$ as $\theta_\infty \to \infty$. In this case the critical values were obtained numerically using $(\overline{D} - a^{*2})\theta^* = R_m^* w_m^*\big|_{\zeta=1}$ in the liquid layer as $R_{m,c}^* = 5.99$ and $a_c^* = 1.09$ for $S = 0.27$.

5. Conclusion

The onset of convection in a binary melt during time-dependent solidification was analyzed. In the mushy layer the near-eutectic solidification model was used for aqueous ammonium chloride solution. In the liquid layer the Lewis number was assumed to be zero and the thermal buoyancy force was neglected. The self-stability equations for the liquid and mushy layers based on the propagation theory were solved numerically. The critical Rayleigh number $R_{m,c}^*$ decreases with increasing the Stefan number *S* and with increasing the Prandtl number *Pr*. When the Stefan number *S* is large, the growth rate of the mushy layer is small. The present model (Eqs. (18) and (19)) for the liquid layer predict a larger critical Rayleigh number $R_{m,c}^*$ than the model of Eq. (24) from Emms and Fowler [9], but when the superheat θ_∞ is very small (the growth rate of the mushy layer is large), the difference of $R_{m,c}^*$ between the two model is very small.

References

1. Fowler, A. C., "The Formation of Freckles in Binary Alloys," *IMA J. Appl. Math.*, **35**(2), 159-174(1985).
2. Glicksman, M. E., Coriell, S. R. and McFadden, G. B., "Interaction of Flows with the Crystal-Melt Interface," *Ann. Rev. Fluid Mech.*, **18**, 307-335(1986).
3. Jones, D. W. R. and Worster, M. G., "Fluxes through Steady Chimneys in a Mushy Layer during Binary Alloy Solidification," *J. Fluid Mech.*, **714**, 127-151(2013).

4. Wells, A. J., Wettlaufer, J. S. and Orszag, S. A., "Nonlinear Mushy-Layer Convection with Chimneys: Stability and Optimal Solute Fluxes," *J. Fluid Mech.*, **716**, 203-227(2013).
5. Worster, M. G., "Instabilities of the Liquid and Mushy Regions during Solidification of Alloys," *J. Fluid Mech*., **237**, 649-669 (1992).
6. Shih, Y. C., Tu, S. M. and Chiu, C. C., "Suppressing Freckles during Solidification due to Periodic Motion of Top Liquid Layer," *Applied Thermal Engineering*, **50**(1), 1055-1069(2013).
7. O'Rourke, J. G., Riggs, A. J. E., Guertler, C. A., Miller, P. W., Padhi, C. M., Popelka, M. M., Wells, A. J., West, A. C., Zhong, J.-Q. and Wettlaufer, J. S., "Mushy-Layer Dynamics in Micro and Hyper Gravity," *Phys. Fluids*, **24**(10), 103305(2012).
8. Tait, S. and Jaupart, C., "Compositional Convection in a Reactive Crystalline Mush and the Evolution of Porosity," *J. Geophys. Res*., **97**, 6735-6756(1992).
9. Emms, P. W. and Fowler, A. C., "Compositional Convection in the Solidification of Binary Alloys," *J. Fluid Mech*., **262**, 111-139 (1994).
10. Choi, C. K., Park, J. H., Park, H. K., Cho, H. J., Chung, T. J. and Kim, M. C., "Temporal Evolution of Thermal Convection in an Initially Stably-Stratified Horizontal Fluid Layer," *Int. J. Thermal Sci.*, **43**(8), 817-823(2004).
11. Kim, M. C. and Choi, C. K., "Some Theoretical Aspects on the Onset of Buoyancy-Driven Convection in a Fluid-Saturated Porous Medium Heated Impulsively from Below," *Korean J. Chem. Eng.*, **32**(12), 2400-2405(2015).
12. Hwang, I. G. and Choi, C. K., "The Onset of Convection in a Mushy Layer during Time-Dependent Solidification," *Proceedings of the 11th International Heat Transfer Conference*, **7**, 193-198 (1998).
13. Hwang, I. G. and Choi, C. K., "The Onset of Mushy-Layer-Mode Instabilities during Solidification in Ammonium Chloride Solution," *J. Crystal Growth*, **220**(3), 326-335(2000).
14. Hwang, I. G. and Choi, C. K., "Onset of Convection in a porous mush during binary Solidification," *Korean J. Chem. Eng.*, **25**(2), 199-202(2008).
15. Hwang, I. G. and Choi, C. K., "Natural Convection during Directional Solidification of a Binary Mixture," *Korean Chem. Eng. Res.*, **47**(2), 174-178(2009).
16. Hwang, I. G., "Stability Analysis of Compositional Convection in a Mushy Layer in the Time-Dependent Solidification System," *Korean J. Chem. Eng.*, **30**(5), 1023-1028(2013).
17. Chung, C. A. and Chen, F., "Onset of Plume Convection in Mushy Layers," *J. Fluid Mech*., **408**, 53-82(2000).
18. Nield, D. A. and Bejan, A., *Convection in porous media*, 4th ed., Springer Science & Business Media, New York, NY(2013).